

Laser Induced Fluorescence Spectroscopy of a Mixed Dimer between 2-Pyridone and 7-Azaindole

Montu K. Hazra,[†] Amit K. Samanta,[‡] and Tapas Chakraborty^{*,†,‡}

Department of Chemistry, Indian Institute of Technology, Kanpur, UP 208016, India, and Department of Physical Chemistry, Indian Association for the Cultivation of Science, Jadavpur, Calcutta 700032, India

Received: March 29, 2007; In Final Form: May 29, 2007

We report here the laser induced fluorescence excitation (FE) and dispersed fluorescence (DF) spectra of a 1:1 mixed dimer between 7-azaindole (7AI) and 2-pyridone (2PY) measured in a supersonic free jet expansion of helium. Density functional theoretical calculation at the B3LYP/6-311++G** level has been performed for predictions of the dimer geometry and normal mode vibrational frequencies in the ground electronic state. A planar doubly hydrogen-bonded structure has been predicted to be the most preferred geometry of the dimer. In the FE spectrum, sharp vibronic bands are observed only for excitation of the 2PY moiety. A large number of low-frequency vibronic bands show up in both the FE and DF spectra, and those bands have been assigned to in-plane hydrogen bond vibrations of the dimer. Spectral analyses reveal Duschinsky-type mixing among those modes in the excited state. No distinct vibronic band structure in the FE spectrum was observed corresponding to excitations of the 7AI moiety, and the observation has been explained in terms of nonradiative electronic relaxation routes involving the 2PY moiety.

1. Introduction

The photophysics and spectroscopy of 7-azaindole (7AI) and 2-pyridone (2PY) dimers have been extensively investigated as prototypes of doubly hydrogen-bonded nucleobase pairs.^{1–26} In the solution phase, UV excitation of 7AI generates green fluorescence and the phenomenon has been interpreted as emission from the excited tautomeric state of a dimeric molecular species. In the excited state, tautomerization within the dimeric molecular adduct occurs via simultaneous exchange of two hydrogen atoms between the two moieties.^{1–2,12} The process has also been studied in the gas phase using various spectroscopic methods^{3,4,6,13–16} and by quantum chemistry calculation at different levels of theory.^{12,17–20}

The gas-phase dimer of 2PY has also attracted a lot of attention in recent years.^{21–26} The binding sites of the species mimic the dimeric adducts of uracil (U) and thymine (T) nucleobases, offering an N–H group as a hydrogen bond donor and an adjacent C=O group as the hydrogen bond acceptor. In the ground state, the molecule (monomer) exists in both the hydroxy (2-hydroxypyridine [2HP]) and keto (2-pyridone) tautomeric forms.^{27,28} Infrared spectroscopic measurement in the gas phase²⁹ reveals that the hydroxy tautomer is more stable than the keto form, and the observation is consistent with the predictions of ab initio quantum chemistry calculations performed in recent years.^{30,31} These calculations also predict that the tautomeric stability is reversed in doubly hydrogen-bonded dimeric species, i.e., the keto form of the dimer is more stable than the hydroxy tautomer,³⁰ and this prediction was found to be consistent with their measured abundances in the electronic spectra of the jet-cooled dimer.^{21–26}

In this paper, we report the laser induced fluorescence spectra (fluorescence excitation as well as dispersed fluorescence) of a

1:1 mixed dimeric complex between 7AI and 2PY. The dimer has been predicted (quantum chemistry calculations) to be stabilized by intermolecular N···H–N and N–H···O type double hydrogen bonds between the two molecular moieties (see below), and it nearly mimics the binding pattern of the A···T and A···U base pairs [A ≡ adenine]. The motivation for investigating this mixed dimeric system is the following. The gap between the S₁ ← S₀ electronic excitation energies of the two molecules in isolated forms is 4808 cm⁻¹.^{3,28} Earlier studies have pointed out that in doubly hydrogen-bonded dimers both chromophores exhibit large spectral shifts in electronic excitation energy. Thus, on homodimer formation 7AI chromophore undergoes ~2300 cm⁻¹ red shift, whereas the (2PY)₂ shows a blue shift of 945 cm⁻¹.^{3,23} These data indicate that, in the present mixed dimer, the lowest electronic transition energy of the 7AI moiety is likely to be more than 1000 cm⁻¹ higher compared to that of the 2PY. Therefore, each moiety can be excited selectively. However, the dynamics of electronic relaxation of the two chromophores in the mixed dimer are expected to be very different. If the 7AI moiety is initially excited, it will behave as an energy donor and 2PY will behave as an acceptor. The hydrogen-bonded dimeric interface will be the spacer. The electronic excitation energy could be transferred from the donor to acceptor mediated by the hydrogen-bonded interface, and the latter would be excited with more than 1000 cm⁻¹ in excess vibronic energy. In a possible second channel, the excited 7AI could be tautomerized via double proton exchange mechanism with the unexcited 2PY moiety, and the latter would be tautomerized simultaneously to the nearly isoenergetic 2-hydroxypyridine (2HP) form. On the other hand, if the 2PY moiety is initially excited, neither the electronic excitation transfer nor tautomeric conversion appears to be energetically feasible. However, for this case, the hydrogen bond characteristics of the dimer can be spectroscopically measured analyzing the low-frequency bands in the emission spectra.

* To whom correspondence should be addressed. Phone: 2473 4971. Fax: (91) (33) 2473 2805. E-mail: pctc@iacs.res.in.

[†] Indian Institute of Technology.

[‡] Indian Association for the Cultivation of Science.

2. Methods

2.1. Experimental Methods. The experimental setup to measure the fluorescence excitation and dispersed fluorescence spectra has been described before.³² Briefly, the carrier gas helium at a pressure of 2 atm was passed successively through a cell containing 7-azaindole at 80 °C temperature and a second glass cell containing 2HP (2-hydroxypyridine) at 100 °C, and the final gas mixture was expanded into a vacuum through a pulsed nozzle (General Valve) of orifice diameter 0.5 mm. The expansion-generated clusters were excited by the frequency-doubled output of a tunable dye laser (Sirah and Plasma Technik, Model Cobra Stretch), which was pumped by the second harmonic ($\lambda = 532$ nm) of a Nd:YAG laser (Spectra Physics, Model INDI). The laser beam (line width ~ 0.5 cm^{-1}) intersects the free jet perpendicularly at about 12 mm downstream of the nozzle orifice, and the emission is collected from the intersection point in a direction perpendicular to both the laser and the free jet. Fluorescence excitation spectra were measured by detecting the total fluorescence by a Hamamatsu R928 photomultiplier tube (PMT). The output signals of the PMT were processed by a boxcar averager (Model RS250, Stanford Research Corporation). The averaged output of the boxcar was stored in a computer using a home-built data acquisition system. To measure the dispersed fluorescence spectra, we have used a 0.75 m monochromator (Spex, Model 750 M) having a grating of groove density 2400/mm and a double staged Peltier cooled ICCD (Jovin Yvon, Model No. 3000V) detector.

2.2. Theoretical Methods. The geometries of 2PY, 7AI, and their 1:1 complex were optimized by the DFT/B3LYP method, and also by ab initio methods at the SCF and MP2 levels using the Gaussian 03 suite of programs.³³ The optimizations were performed without any symmetry restriction. For the DFT/B3LYP method, 6-311++G** and 6-311++G (2d,2p) basis sets were used. A recent study on hydrogen-bonded DNA base pairs shows that the geometric and energetic parameters calculated using the PW91 functional satisfactorily match those predicted by the RI-MP2 method at Sponer's complete basis set (CBS) extrapolation limit.³⁴ On the other hand, the vibrational frequencies and particularly the low-energy intermolecular modes of hydrogen-bonded dimeric complexes calculated by the B3LYP/6-311++G** method show excellent agreement with the experimentally measured values.^{23,26,31,35–37} We also have performed the DFT calculation at the PW91/6-311++G** level for both geometry optimization and prediction of normal mode frequencies of the 7AI \cdots 2PY dimer. Basis set superposition errors (BSSEs) in the calculated binding energies (E_{HB}) of the complex have been corrected by the counterpoise (CP) method of Boys and Bernardi.³⁸

3. Results and Discussion

3.1. Experimental Results. *3.1.A. Fluorescence Excitation Spectra.* The fluorescence excitation (FE) spectrum of the dimer has been measured by exciting both the 7AI and 2PY moieties. The electronic origin bands for the $S_1 \leftarrow S_0$ transition of the two isolated molecules appear at 34 639 and 29 831 cm^{-1} , respectively.^{3,28} Quantum chemistry calculation (presented below) predicts that the most preferred binding pattern is a planar doubly hydrogen-bonded linkage, similar to that in the homodimers of 2PY and reactive dimer of 7AI.^{17,26} Therefore, to record the FE spectrum corresponding to local excitation of the 2PY moiety, the laser frequency was tuned in the 2PY homodimer absorption region. A section of this spectrum in the span of 750 cm^{-1} is presented in Figure 1. Here the most intense band at the lowest transition energy (30 596 cm^{-1}) has been

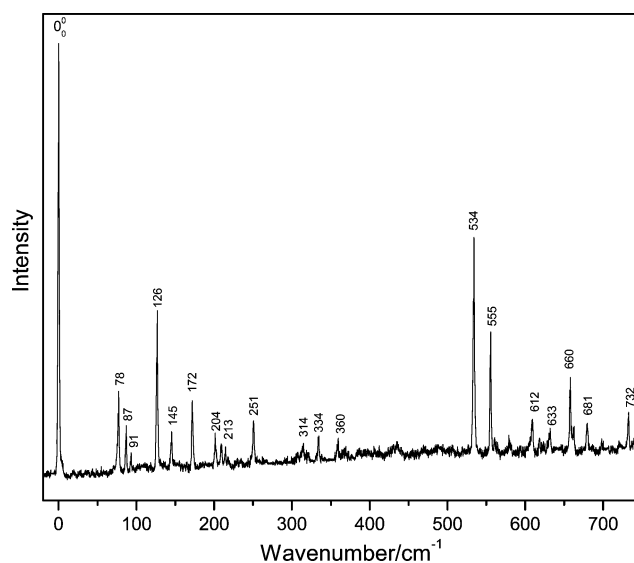


Figure 1. Fluorescence excitation spectrum for $S_1 \leftarrow S_0$ electronic transition of 7AI \cdots 2PY mixed dimer in a supersonic free jet expansion. The electronic origin band at 30 596 cm^{-1} has been considered as the zero of the frequency (cm^{-1}) scale. Assignments of major intermolecular vibronic bands have been discussed in the text.

assigned to the electronic origin band of the dimer, and it is 765 cm^{-1} blue-shifted from the 2PY monomer origin ("A" origin).²⁸ This transition frequency can be compared with the 0_0^0 origin position of 2PY homodimer, which appears at 30 776 cm^{-1} . This homodimer origin is 945 cm^{-1} blue-shifted from the 2PY monomer origin transition frequency.²⁴ Incidentally, this band of the 2PY homodimer has been assigned to the allowed upper exciton component.²⁵ Thus, the origin of the 2PY–7AI dimer is red-shifted by 180 cm^{-1} relative to the origin of the (2PY)₂ homodimer. In other words, the allowed lowest energy electronic transition of 2PY moiety is less blue-shifted in 2PY–7AI mixed dimer compared to that in the (2PY)₂ homodimer. This is possibly because of somewhat smaller binding energy (hydrogen bond energy) of the mixed dimer compared with that of the homodimer.

The most significant feature of the spectrum in Figure 1 is the appearance of a large number of low-frequency vibronic bands, e.g., the bands at 78, 87, 91, 126, 145, and 172 cm^{-1} . The lowest energy vibronic band in the FE spectrum of 2PY monomer shows up at 217 cm^{-1} excess energy of the S_1 origin.²⁸ By changing the backing pressures of carrier gas and the sample concentration in the preexpansion gas mixture, we have noticed that the relative intensities of the bands in Figure 1 remain practically unaltered. Therefore, we conclude that all the bands in the spectrum are cold and that they belong to the $S_1 \leftarrow S_0$ absorption system of 7AI \cdots 2PY mixed dimeric complex. The low-frequency bands in the spectrum must be due to different intermolecular vibrations in the excited state. We have suggested assignments of these bands from analyzing the fluorescence spectra recorded following single vibronic level excitations as presented below. It is noteworthy that, unlike 2PY homodimer, we did not notice a rapid drop in intensity of the vibronic bands appearing beyond 500 cm^{-1} excess energy in the S_1 potential energy surface.²³ However, the dispersed fluorescence (DF) spectra recorded following vibronic excitations of the intramolecular vibronic bands of 2PY ring (534, 555 cm^{-1} , etc.) do not show much-structured features.

In the second step, we attempted to record the FE spectrum of the dimer by exciting the 7AI moiety. For this purpose we scanned the laser frequency in the $S_1 \leftrightarrow S_0$ absorption region

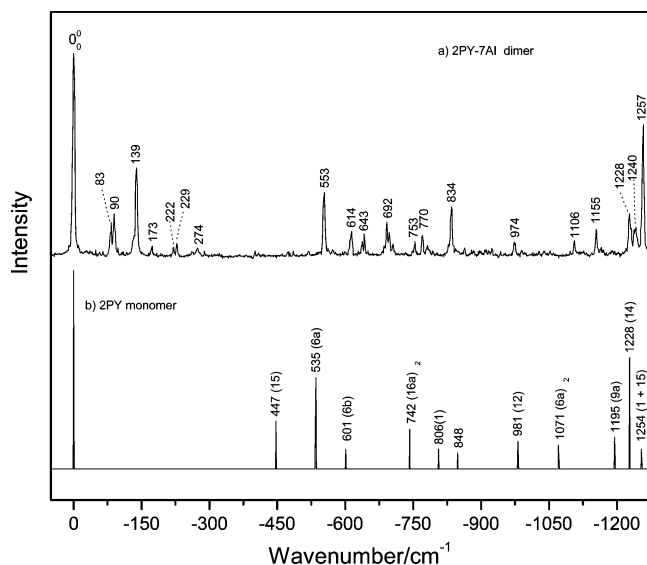


Figure 2. Comparison between the dispersed fluorescence spectra of 7AI••2PY mixed dimer (a) measured by exciting the $S_1 \leftarrow S_0$ origin band and the same for 2PY monomer (b) as reported in ref 28. The latter has been reproduced here in stick spectral format.

of the 7AI homodimer. However, except for some broad features over a continuous background, we could not identify any distinct peak, which can be confidently corresponded to vibronic features arising due to excitations of the 7AI moiety. To verify the fluorescence characteristics of 7AI in such a dimeric environment, we recorded the FE spectrum of a 1:1 mixed dimer of 7AI with formamide (FM).³⁹ The hydrogen-bonding sites of FM are similar to those of 2PY. A DFT theoretical calculation at the B3LYP/6-311++G** level predicts that the most preferred binding pattern of FM with 7AI is also the doubly hydrogen-bonded type. In our measured FE spectrum, 7AI••FM dimer shows only regular sharp vibronic features. Its 0_0^0 transition, which can be localized only on the 7AI moiety, appears at $32\,335\text{ cm}^{-1}$ and is only 69 cm^{-1} blue-shifted from the origin band of 7AI homodimer band ($32\,266\text{ cm}^{-1}$). This observation guided us to search the vibronic bands corresponding to excited 7AI moiety of the 7AI••2PY dimer. However, the absence of distinct band structure indicates that the electronic energy from the excited 7AI moiety of the dimer is nonradiatively dissipated through an effective involvement of the 2PY moiety. As mentioned before, an apparent dissipation channel is the electronic excitation energy transfer from the 7AI to the PY moiety. In such a case, 2PY will be excited to a higher lying singlet state and that can decay nonradiatively by an intersystem-crossing process. Alternatively, such intersystem crossing can also occur from the excited 7AI mediated through the hydrogen-bonded interface of the dimer.^{40,41} Such a process cannot happen if 2PY is replaced by FM. The second nonradiative decay channel could be the tautomeric conversion via simultaneous transfer of two hydrogen atoms along the hydrogen bonds of the dimeric interface. In this case, 2PY will be tautomerized simultaneously to 2HP in the ground electronic state. In such an event, the electronically excited tautomeric form of 7AI, the dimer of which exhibits green fluorescence in solutions,¹ can decay nonradiatively in the gas phase by an intersystem-crossing process.

3.1.B. Dispersed Fluorescence Spectra. (i) 0_0^0 Excitation. The first $\sim 1300\text{ cm}^{-1}$ of the dispersed fluorescence (DF) spectrum measured following excitation of the 0_0^0 origin band of the 2PY moiety of the dimer is presented in Figure 2. The frequencies of the major bands and their assignments are

TABLE 1: Assignments of the Vibronic Bands in the DF Spectrum of 7AI••2PY Dimer Measured by Exciting the $S_1 \leftarrow S_0$ Electronic Origin Band^a

7AI••2PY		assignment
observed (cm^{-1})	predicted (cm^{-1})	
0		origin
83	80	opening (X_1^0)
90	98	shearing (Y_1^0)
139	137	H-bond stretching (Z_1^0)
173		$(X_1^0 + Y_1^0)$
222		$(Z_1^0 + X_1^0)$
229		$(Z_1^0 + Y_1^0)$
274		Z_2^0
553	561	6a
614	625	6b
636		$6a + X_1^0$
643		$6a + Y_1^0$
692		$6a + Z_1^0$
753		$6b + Z_1^0$
770	398	$16a_2^0$
834	841	1
974		$1 + Z_1^0$
1106		$6a_2^0$
1155	1171	9b
1228		$6b_2^0$ (?)
1240	1241	9a
1257	1270	14

^a The frequencies of the observed bands tabulated here are with respect to the 0_0^0 band of the dimer ($30\,596\text{ cm}^{-1}$).

presented in Table 1. Varsanyi nomenclature⁴² of monosubstituted benzene derivatives has been used to denote the vibronic fundamentals. Assignments of the bands have been suggested by comparing the observed frequencies with the normal mode frequencies predicted by the DFT/B3LYP/6-311++G** level of calculation.

A stick diagram of the origin-excited DF spectrum of 2PY monomer is presented in Figure 2b. It shows that the first prominent vibronic band appears at 447 cm^{-1} displacement from the excitation frequency.²⁸ In contrast, the dimer spectrum in Figure 2 shows many distinct bands below this frequency and the features are similar to what appear in the FE spectrum. We associate these low-frequency bands to intermolecular vibrational frequencies of the dimer. The pictures of six such normal mode vibrations, predicted by the DFT/B3LYP/6-311++G** level of calculation, are presented in Figure 3. It is seen that the predicted vibrational frequencies of all such modes are below 200 cm^{-1} . A comparison between the experimental and theoretical frequencies is presented in Table 1. On the basis of this comparison, we assign the two weak bands at 83 and 90 cm^{-1} in Figure 2 to the in-plane opening and shearing vibrations, respectively; the corresponding predicted frequencies are 80 and 98 cm^{-1} . The combination of these two fundamentals appears at 173 cm^{-1} . The strongest low-frequency band in the spectrum at 139 cm^{-1} is assigned to hydrogen bond stretching fundamental, and the overtone transition appears at 274 cm^{-1} . The predicted intermolecular stretching vibrational frequency is 137 cm^{-1} . The doublet bands at 222 and 229 cm^{-1} can be assigned as the combination of hydrogen bond stretching fundamental (139 cm^{-1}) with the in-plane opening (83 cm^{-1}) and shearing (90 cm^{-1}) fundamentals.

The vibronic bands at 553 , 614 , 834 , and 1257 cm^{-1} in Figure 2a have been assigned to different fundamentals of the intramolecular in-plane modes of the 2PY moiety of the dimer. We assign these bands to benzenoid $6a_1^0$, $6b_1^0$, 1_1^0 , and 14_1^0 transitions, respectively, of the 2PY ring and the corresponding

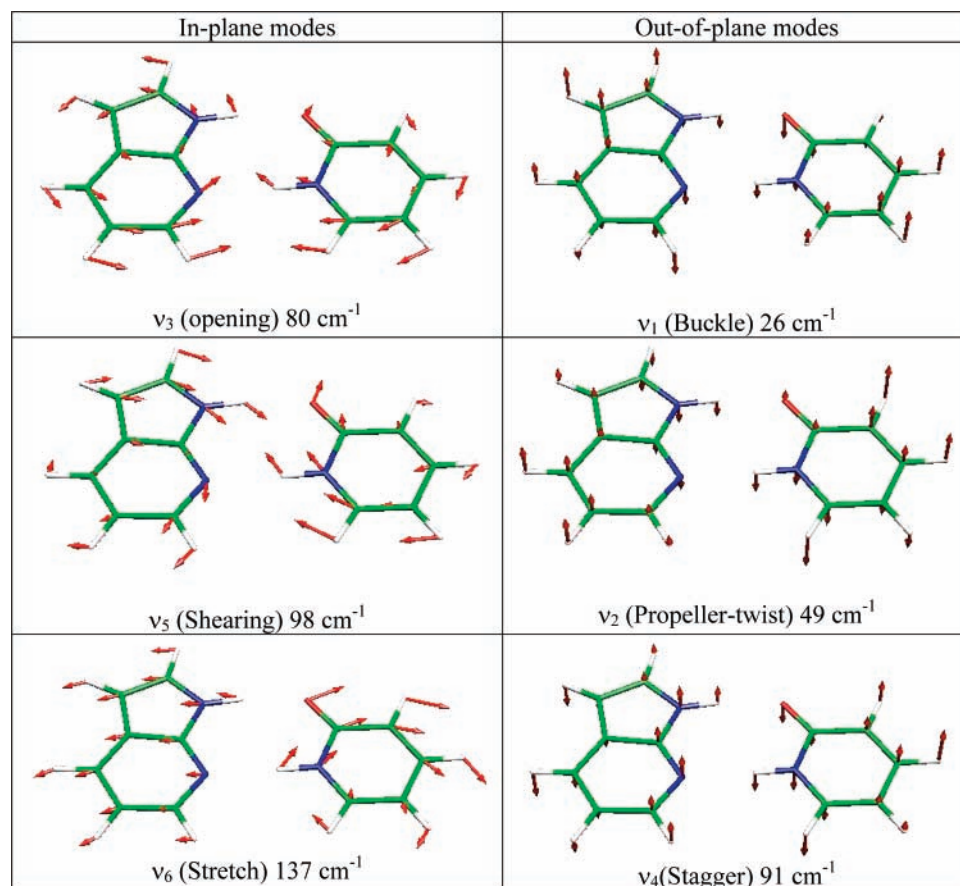


Figure 3. Normal modes of the six intermolecular vibrations of the 7AI \cdots 2PY mixed dimer calculated at the B3LYP/6-311++G** level of theory.

calculated frequencies are 561, 625, 841, and 1270 cm^{-1} . The weak band at 770 cm^{-1} has been assigned to the overtone of 16a transition ($16a_2^0$). Other bands in the spectrum can be interpreted as combinations of these fundamentals with the low-frequency bands.

(ii) Excitations of Low-Frequency Bands. The DF spectra were recorded by exciting the $0_0^0 + 77$, 87 , and 126 cm^{-1} bands. The first 500 cm^{-1} of these spectra are shown in Figure 4, and the origin-excited DF spectrum in the same energy range is also shown here (Figure 4a) for comparison. It is seen that the prominent low-frequency bands in the first three spectra (Figure 4b–d) are also present in the origin-excited DF spectrum, but the relative intensities of these bands in all four spectra are different. Thus, in Figure 4b the band at 83 cm^{-1} is enhanced compared to the adjacent 90 cm^{-1} band, although in Figure 4a they are nearly equally intense. We already have assigned these two frequencies to in-plane opening and shearing modes of the hydrogen bond interface. In addition, prominent vibronic bands are seen also at 165, 173, and 222 cm^{-1} . In the DF spectrum of the electronic origin (Figure 4a), the latter two appear weakly and have been assigned to combinations of the opening with shearing and stretching vibration, respectively. Therefore, these bands are definitely cross-sequence type transitions and their appearances are indications of extensive mixing of the low-frequency modes; this happens due to in-plane deformation of the hydrogen-bonding frame of the dimer. The 165 cm^{-1} band can be assigned as an overtone of the 83 cm^{-1} band, and it is completely absent in Figure 4a. The cross-sequence stretching fundamental at 139 cm^{-1} appears very weakly, but combination of the stretching with shearing (90 cm^{-1}) appears quite prominently at 229 cm^{-1} .

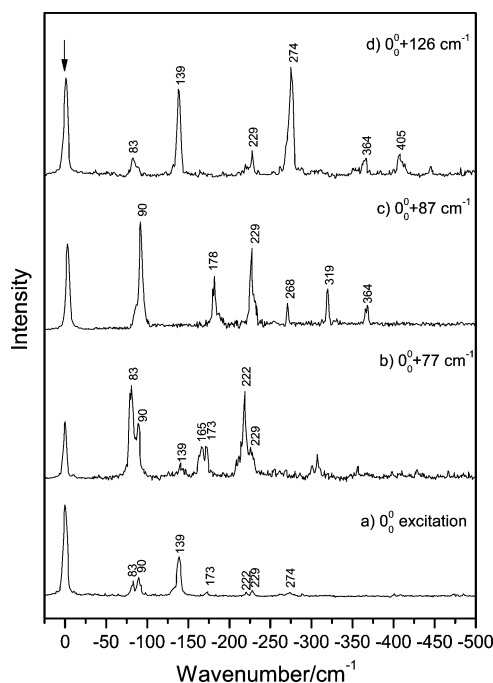


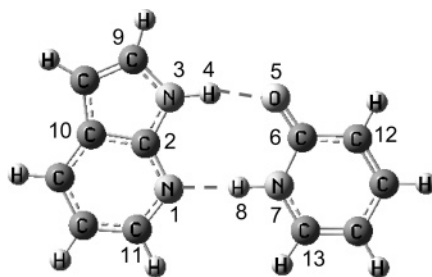
Figure 4. Resolved fluorescence spectrum following excitations of the (a) 0_0^0 , (b) $0_0^0 + 78\text{ cm}^{-1}$, (c) $0_0^0 + 87\text{ cm}^{-1}$, and (d) $0_0^0 + 126\text{ cm}^{-1}$ bands of 7AI \cdots 2PY.

The DF spectrum for excitation of the $0_0^0 + 87\text{ cm}^{-1}$ band excess energy (Figure 4c) shows a three-member progression (Y_1^1 , Y_2^1 , and Y_3^1) for the shearing mode, and the corresponding bands appear at 90, 178, and 268 cm^{-1} . The bands at 229, 319, and 364 cm^{-1} can be assigned as the following combinations:

TABLE 2: Optimized Bond Lengths (angstroms) and Bond Angles (deg) of 7AI...2PY Mixed Dimer at Different Levels of Theoretical Calculation

$$R_1 \equiv N_1 \cdots N_7$$

$$R_2 \equiv N_3 \cdots O_5$$



geom params	7AI...2PY				
	2PY B3LYP/6-311++G**	7AI B3LYP/6-311++G**	B3LYP/6-311++G**	MP2/6-31G**	PW91/6-311++G**
$N_1 \cdots N_7$			2.96	2.91	2.88
$N_3 \cdots N_5$			2.81	2.79	2.76
N_1-C_2		1.33	1.34	1.34	1.34
C_2-N_3		1.37	1.37	1.37	1.37
N_3-H_4		1.00	1.03	1.03	1.04
H_4-O_5			1.79	1.77	1.72
O_5-C_6	1.22		1.24	1.25	1.25
C_6-N_7	1.41		1.39	1.39	1.40
N_7-H_8	1.01		1.04	1.04	1.06
H_8-N_1			1.92	1.88	1.82
$N_1-C_2-N_3$		125.6	125.7	125.2	125.4
$C_2-N_3-H_4$		124.3	123.9	123.8	123.4
$N_3-H_4-O_5$			169.0	171.4	170.4
$H_4-O_5-C_6$			129.1	125.8	127.6
$O_5-C_6-N_7$	120.0		120.6	121.4	120.6
$C_6-N_7-H_8$	114.4		117.1	117.3	117.6
$N_7-H_8-N_1$			179.2	178.9	179.7
$H_8-N_1-C_2$			115.3	114.0	115.1
$N_1-C_2-C_{10}$		127.0	126.0	126.4	126.2
$H_4-N_3-C_9$		126.6	127.7	127.9	128.3
$N_3-C_2-C_{10}$		107.4	108.2	108.3	108.4
$O_5-C_6-C_{12}$	126.9		125.0	124.6	124.8
$N_7-C_6-C_{12}$	113.1		114.4	114.0	114.5
$H_8-N_7-C_{13}$	120.2		118.7	117.9	118.3
$C_2-N_1 \cdots N_7-C_6$			0.000	0.000	0.000
$C_{11}-N_1 \cdots N_7-C_{13}$			0.000	0.000	0.000
$C_2-N_3 \cdots O_5-C_6$			0.000	0.000	0.000

$90 + 139 (Y_1^1 Z_1^0) \text{ cm}^{-1}$, $90 + 229 (Y_2^1 + Z_1^0) \text{ cm}^{-1}$, and $90 + 274 (Y_1^1 + Z_2^0) \text{ cm}^{-1}$, respectively. Thus, the frequency of the shearing mode appears to exhibit a small shift (90 to 87 cm^{-1}) on $S_0 \rightarrow S_1$ excitation.

Figure 4d shows the DF spectrum recorded following excitation of the $0_0^0 + 126 \text{ cm}^{-1}$ band. The sequence origin appears at 139 cm^{-1} displacement, and the two overtone transitions appear at 274 and 405 cm^{-1} . Thus, on $S_1 \leftarrow S_0$ excitation, the stretching frequency appears to decrease by 13 cm^{-1} . The cross-sequence transitions for shearing (83 cm^{-1}) and opening (90 cm^{-1}) vibrations and their combination with the stretching fundamental also show up in the spectrum.

We attempted to measure the DF spectra of the other low-frequency features appearing in the FE spectrum. However, because of low signal level, we could not record those spectra with a reasonable signal-to-noise ratio.

3.2. Theoretical Results. For initial prediction of possible isomeric structures of the dimer, we calculated the electrostatic potential maps of the two molecules. Among the different possible dimer geometries, the doubly hydrogen-bonded structure was found to be the most stable. A few selected calculated geometric parameters of the dimer are presented in Table 2. It is seen that the dimer formation significantly alters the C=O and C-N bond lengths and also the bond angles adjacent to

the hydrogen bonds of both molecules. For example, according to the DFT/B3LYP/6-311++G** calculation, the $\angle C_2-N_3-H_4$ and $\angle N_1-C_2-C_{10}$ bond angles of 7AI are altered from 124.3 and 127.0° in the monomer to 123.9 and 126.0° in the dimer. Similarly, the $\angle C_6-N_7-H_8$, $\angle O_5-C_6-C_{12}$, and $\angle H_8-N_7-C_{13}$ bond angles are altered from 114.4 , 126.9 , and 120.2° in 2PY monomer to 117.1 , 125.0 , and 118.7° in the mixed dimer. Such deformation in geometric parameters indicates that vibrational modes involving the motions of 2PY ring atoms are likely to be somewhat different compared to those of the isolated molecule. This expectation is also reflected in the calculated ground state normal vibrational mode frequencies.

The BSSE corrected binding energies of the dimer (D_e) predicted by MP2/6-31G**, B3LYP/6-311++G**, B3LYP/6-311++G (2d,2p), and PW91/6-311++G** calculations are 16.92 , 15.42 , 15.08 , and 17.93 kcal/mol , respectively, and the corresponding uncorrected values are 21.75 , 16.09 , 15.48 , and 18.81 kcal/mol . Thus, nearly 5 kcal/mol BSSE correction for the MP2/6-31G** calculation is a clear indication of a lower basis set effect. Because of our limited computational resources, we could not perform geometry optimization using higher basis sets at the MP2 level of calculation.

The predicted geometric parameters indicate that the mixed dimer is completely planar in the ground state, although the

lengths of the two hydrogen bonds ($R_1 \equiv \text{N}_1 \cdots \text{N}_7$ and $R_2 \equiv \text{N}_3 \cdots \text{O}_5$) appear quite different. At the B3LYP/6-311++G** level, the values of R_1 and R_2 are 2.96 and 2.81 Å, respectively, and for the 6-311++G(2d,2p) basis set those two lengths are predicted to be 2.95 and 2.80 Å. The bond lengths calculated at the MP2/6-31G** and PW91/6-311++G** levels appear shorter compared to the values predicted at the DFT/B3LYP level of calculation. The R_1 and R_2 values are 2.91 and 2.79 Å at the MP2/6-31G** calculation and 2.88 and 2.76 Å, respectively, at the PW91/6-311++G** level of calculation.

To assess the reliability of the geometric parameters predicted by the above-mentioned calculations, we have repeated the same on 2PY homodimer, because for this species the geometric parameters from high-resolution spectroscopic measurements and the binding energy value predicted by a much higher level of theoretical calculation are available in the literature.²⁶ Thus, the N \cdots O distance along the hydrogen bonds in (2PY)₂ predicted by the DFT/B3LYP/6-311++G** level of calculation (2.780 Å) shows excellent agreement with the experimentally measured value (2.77 Å). A similar agreement has also been found in the case of the intermolecular vibrational frequencies between the measurement and calculation. In comparison, the bond lengths calculated by MP2 and PW91 methods using the same basis set are 2.735 and 2.730 Å, respectively, and these values are shorter compared to the experimental value. The binding energy (D_e) predicted by CCSD(T) method at the CBS limit is 21.9 kcal/mol, and this can be compared with the values predicted by DFT/B3LYP/6-311++G** and PW91/6-311++G** methods, 19.5 and 21.7 kcal/mol, respectively.

4. Summary and Conclusion

We have presented here vibronically resolved electronic spectra for $S_1 \leftrightarrow S_0$ transitions of a doubly hydrogen-bonded mixed dimer between 2-pyridone and 7-azaindole. The fluorescence excitation spectrum recorded following excitation of the 2PY moiety of the jet-cooled dimer exhibits low-frequency vibronic bands corresponding to hydrogen bond modes at the dimeric interface. Assignments of these bands have been suggested from measurement of their dispersed fluorescence spectra and normal mode vibrational frequencies calculated using the DFT/B3LYP/6-311++G** theoretical method. The emission spectra also indicate that the in-plane intermolecular vibrations undergo Duschinsky-type mode mixing in the S_1 state. Discrete vibronic structures in the emission spectra disappeared when the intramolecular modes of the 2PY ring of frequencies exceeding 534 cm⁻¹ were excited.

We also tried to measure the FE spectrum of the dimer by exciting the 7AI moiety. However, we could not record discrete vibronic structures in the spectrum. On the other hand, structured spectra were recorded in the same spectral region in the case of a 1:1 dimer of 7AI with formamide, wherein the intermolecular binding motif, according to quantum chemistry calculation, is similar to that of the 7AI \cdots 2PY dimer. This observation indicates that the 2PY moiety of the dimer plays an effective role in rapid nonradiative relaxation of excited 7AI in the dimer, and we have tentatively proposed two probable mechanisms for the radiationless dissipation of the electronic energy.

Acknowledgment. The authors gratefully acknowledge the financial support received from the department of science and technology, Government of India, to carry out the research. M.K.H. and A.K.S. acknowledge CSIR, Government of India, for senior research fellowships.

References and Notes

- (1) Taylor, C. A.; El-Bayoumi, M. A.; Kasha, M. M. *Proc. Natl. Acad. Sci. U.S.A.* **1969**, *63*, 253.
- (2) Ingham, K. C.; Abu-Elgheit, M.; El-Bayoumi, M. A. *J. Am. Chem. Soc.* **1971**, *93*, 5023.
- (3) Fuke, K.; Yoshiuchi, H.; Kaya, K. *J. Phys. Chem.* **1984**, *88*, 5840.
- (4) Fuke, K.; Kaya, K. *J. Phys. Chem.* **1989**, *93*, 614.
- (5) Nakajima, A.; Ono, F.; Kihara, Y.; Ogawa, A.; Matsubara, K.; Ishikawa, K.; Baba, M.; Kaya, K. *Laser Chem.* **1995**, *15*, 167.
- (6) Douhal, A.; Kim, S. K.; Zewail, A. H. *Nature* **1995**, *378*, 260.
- (7) Nakajima, A.; Hirano, M.; Hasumi, R.; Kaya, K.; Watanabe, H.; Carter, C. C.; Williamson, J. M.; Miller, T. A. *J. Phys. Chem. A* **1997**, *101*, 392.
- (8) Lopez-Martens, R.; Long, P.; Solgadi, D.; Soep, B.; Syage, J.; Millie, P. *Chem. Phys. Lett.* **1997**, *273*, 219.
- (9) Catalan, J.; Pérez, P.; del Valle, J. C.; Kasha, M. *Proc. Natl. Acad. Sci. U.S.A.* **1999**, *96*, 8338.
- (10) Yokoyama, H.; Watanabe, H.; Omi, T.; Ishiuchi, S.; Fujii, M. *J. Phys. Chem. A* **2001**, *105*, 9366.
- (11) Sakai, M.; Ishiuchi, S.; Fujii, M. *Eur. Phys. J. D* **2002**, *20*, 399.
- (12) Catalan, J.; Pérez, P.; del Valle, J. C.; de Paz, J. L. G.; Kasha, M. *Proc. Natl. Acad. Sci. U.S.A.* **2004**, *101*, 419.
- (13) Sakota, K.; Hara, A.; Sekiya, H. *Phys. Chem. Chem. Phys.* **2004**, *6*, 32.
- (14) Sakota, K.; Sekiya, H. *J. Phys. Chem. A* **2005**, *109*, 2718.
- (15) Sakota, K.; Sekiya, H. *J. Phys. Chem. A* **2005**, *109*, 2722.
- (16) Sakota, K.; Okabe, C.; Nishi, N.; Sekiya, H. *J. Phys. Chem. A* **2005**, *109*, 5245.
- (17) Catalan, J.; Pérez, P.; del Valle, J. C.; de Paz, J. L. G.; Kasha, M. *Proc. Natl. Acad. Sci. U.S.A.* **2002**, *99*, 5793.
- (18) Catalan, J.; Pérez, P.; del Valle, J. C.; de Paz, J. L. G.; Kasha, M. *Proc. Natl. Acad. Sci. U.S.A.* **2002**, *99*, 5799.
- (19) Serrano-Andrés, L.; Merchán, M. *Chem. Phys. Lett.* **2006**, *418*, 569.
- (20) Gelabert, R.; Moreno, M.; Lluch, J. M. *J. Phys. Chem. A* **2006**, *110*, 1145.
- (21) Held, A.; Pratt, D. W. *J. Am. Chem. Soc.* **1990**, *112*, 8629.
- (22) Held, A.; Pratt, D. W. *J. Chem. Phys.* **1992**, *96*, 4869.
- (23) Müller, A.; Talbot, F.; Leutwyler, S. *J. Chem. Phys.* **2000**, *112*, 3717.
- (24) Matsuda, Y.; Ebata, T.; Mikami, N. *J. Chem. Phys.* **2000**, *113*, 573.
- (25) Müller, A.; Talbot, F.; Leutwyler, S. *J. Chem. Phys.* **2002**, *116*, 2836.
- (26) Müller, A.; Losada, M.; Leutwyler, S. *J. Phys. Chem. A* **2004**, *108*, 157.
- (27) Beak, P.; Fry, F. S. *J. Am. Chem. Soc.* **1973**, *95*, 1700.
- (28) Nimlos, M. R.; Kelley, D. F.; Bernstein, E. R. *J. Phys. Chem.* **1989**, *93*, 643.
- (29) Nowak, M. J.; Lapinski, L.; Fulara, J.; Les, A.; Adamowicz, L. *J. Phys. Chem.* **1992**, *96*, 1562.
- (30) Fu, A.; Li, H.; Du, D.; Zhou, Z. *J. Phys. Chem. A* **2005**, *109*, 1468.
- (31) Hazra, M. K.; Chakraborty, T. *J. Phys. Chem. A* **2006**, *110*, 9130.
- (32) Das, A.; Mahato, K. K.; Chakraborty, T. *J. Chem. Phys.* **2001**, *114*, 6107.
- (33) Frisch, M. J.; Trucks, G. W.; Schlegel, H. B.; et al. *Gaussian 03*, revision B.05; Gaussian Inc.: Pittsburgh, PA, 2003.
- (34) van der Wijst, T.; Guerra, C. F.; Swart, M.; Bickelhaupt, F. M. *Chem. Phys. Lett.* **2006**, *426*, 415.
- (35) Müller, A.; Talbot, F.; Leutwyler, S. *J. Chem. Phys.* **2001**, *115*, 5192.
- (36) Müller, A.; Talbot, F.; Leutwyler, S. *J. Am. Chem. Soc.* **2002**, *124*, 14486.
- (37) Hazra, M. K.; Samanta, A. K.; Chakraborty, T. *J. Chem. Phys.* **2006**, *125*, 214302.
- (38) Boys, S. F.; Bernardi, F. *Mol. Phys.* **1970**, *19*, 553.
- (39) Hazra, M. K.; Chakraborty, T. Manuscript in preparation.
- (40) Amirav, A.; Sonnenschein, M.; Jortner, J. *Chem. Phys. Lett.* **1983**, *100*, 488.
- (41) Chattoraj, M.; Chung, D. D.; Paulson, B.; Closs, G. L.; Levy, D. H. *J. Phys. Chem.* **1994**, *98*, 3361.
- (42) Varsanyi, G. *Vibrational spectra of Benzene Derivatives*; Academic: New York, 1969.